# Laser Dazzling of Focal Plane Array Cameras

Ric (H.)M.A. Schleijpen[1], Alwin Dimmeler[2], Bernd Eberle[2], Johan C. van den Heuvel[1], Arjan L. Mieremet[1], Herman Bekman[1], Benoit Mellier[3].
[1]TNO Defence, Security and Safety, P.O. Box 96864, 2509 JG The Hague, The Netherlands,
[2]FGAN-FOM Gutleuthausstrasse 1, 76275 Ettlingen, Germany,
[3]CELAR, Division DIRAC, 35170 Bruz, France.

**ABSTRACT**

Laser countermeasures against infrared focal plane array cameras aim to saturate the full camera image. In this paper we will discuss the results of dazzling experiments performed with MWIR lasers. In the "low energy" pulse regime we observe an increasing saturated area with increasing power. The size of the saturated area can be explained by an expression derived from the point spread function of the optics.
The experimental results for short "high energy" pulses show a strong non-linear response of the detector arrays. Physical processes potentially responsible for these effects are described. Possible consequences of this non-linear detector behaviour for the effectiveness of laser countermeasures applying short high energy pulses are discussed. A better understanding of the response of infrared detectors to short high energy laser pulses, will allow changing the laser design in order to mitigate these effects.

**Keywords:** Laser dazzling, Focal plane array cameras, Countermeasures, Infrared, Non-linear detector response.

## 1. INTRODUCTION

Recent developments in laser technology have made several options available for MWIR lasers for the use in Infrared Countermeasure systems. Well known examples of these systems are Directed Infrared Countermeasure (DIRCM) systems, mounted on board of aircraft for platform self protection. DIRCM systems are primarily designed for use against current anti-aircraft missiles, based on reticule or scanning detector technology. Using the appropriate jam codes, this generation of infrared seekers can be deceived. However, the next generation infrared missiles will use imaging seekers. When these seekers use focal plane array detectors, deception is no longer possible while dazzling with a continuous laser source is considered a potential countermeasure in that case. Dazzling with a continuous or quasi-continuous pulsed laser causes a reversible saturation effect on the detector array. Since we are explicitly interested in the detector response in the saturation range we select the detector operating conditions accordingly and do not allow automatic gain corrections, although the automatic gain correction is traditionally vulnerable to countermeasures. Permanent damage effects which require much higher irradiance levels than dazzling effects are also outside the scope of this paper. This is because most of the current MWIR lasers provide irradiance levels, which do not exceed dazzling effects at ranges between a few hundred to a few thousand meters. The countermeasure application of MWIR lasers is not limited to missile seekers. Therefore, we will discuss the laser countermeasure effects of DIRCM like laser systems on imaging systems in general. In a previous paper we have discussed laser dazzling effects on cameras in detail (reference 1). Reference 1 discussed the relation between the size of the saturated area in the image and the laser power incident on the entrance pupil of the optics. The growth of the saturated area is purely related to optical effects and can be described mathematically using the diffraction limited point spread function. In this paper we will have closer look at the effects at very high intensities and very short pulses. We use partially the same data set as in reference 1 supplemented by some additional experiments.

The paper is organised as follows; in section 2 we start with a description of three different experimental set-ups that have been used for data collection. In section 3 we will discuss the experimental results for the dazzling experiments and discuss some observations of non-linear detector response to high energy pulses. Section 4 will present considerations on saturation mechanisms which could be responsible for the non-linear detector response. Section 5 will discuss the consequences of these effects for the effectiveness of countermeasure lasers and we finish with our main conclusions in section 6.

ric.schleijpen@tno.nl, phone +31 70 374 0045, fax +31 70 374 0654, www.tno.nl

Technologies for Optical Countermeasures IV, edited by David H. Titterton, Mark A. Richardson
Proc. of SPIE Vol. 6738, 67380O, (2007) · 0277-786X/07/$18 · doi: 10.1117/12.747009

## 2. EXPERIMENTAL SET-UP

Experiments were performed with three different combinations of infrared focal plane array cameras and MWIR lasers. A CMT camera is used in combination with a DF laser and a frequency doubled $CO_2$ laser and an InSb camera is used with a PPLN-OPO laser. Each of the three set-ups was used at a different location, with different ranges between camera and laser.

### 2.1. CMT camera with DF laser

The CMT camera is an infrared imaging seeker simulator system as illustrated in figure 1. A detailed description is given in reference 2. The system is basically an infrared camera with a unit for steering the field of view. The field of view of the camera is 4.4° x 4.4° covered by a 256 x 256 detector array with snap-shot read-out. During all laser tests, the camera had a fixed 1 ms integration time and 100 Hz frame rate for the detector array. The field of view is steered by a Risley prism unit similar to the steering unit described in reference 3. This field-of-view steering unit adds extra optical elements to the system, which may cause scatter effects in the optics to appear stronger than in usual camera optics. The Risley prisms alone add eight optical elements, not counting the additional correction lenses required in this optical design. For all the tests the laser was aligned along the seeker bore-sight in order to avoid ghost images which could disturb the interpretation of the test results.

Figure 1: Imaging Seeker Simulator including the CMT camera

The DF chemical laser is a CW laser modulated by an acousto-optic cell. The laser combined with calibrated attenuators enabled to generate controlled levels of CW laser output or controlled laser pulse sequences like in an infrared jammer. For a more complete description of the experimental set-up see reference 2. During the experiments, the laser was operated both in CW mode and pulse mode, the latter with various pulse frequencies (5 and 20 kHz) and various pulse durations between 5 μs and 100 μs. This allowed analysing the effects of "long" pulses on the CMT detector array.

The laser irradiance levels on the seeker varied from $10^4$ pW/cm$^2$ to $10^7$ pW/cm$^2$. This range covers typical DIRCM laser irradiance levels on seekers, taking into account typical values for the laser power, the laser beam divergence and the engagement range. The upper level was selected to avoid damage to the detector. Both laser and camera were mounted on an optical test bench for the experiments at a few meters distance.

### 2.2. InSb camera and PPNL OPO laser

The InSb camera is a standard 256 x 320 array camera with narrow (1.5° x 2.0°) and wide (4.5° x 6.0°) field of view optics. The camera is used at a fixed integration time and standard NTSC frame rate.

The laser is a PPLN OPO laser pumped by a Nd:$YVO_4$ laser as described in reference 4. The laser wavelength used in the experiments is around 3.9 μm. The pulse repetition frequency is determined by the PRF of the pump laser which is set to 30 kHz. This pulse rate ensures that a significant number of pulses are emitted within the camera integration time of typically 1 ms. The MWIR laser pulse length is determined by the pulse length of the pump laser, which was

measured to be between 8 and 9 ns at 30 kHz. The actual emitted pulse could be slightly shorter, because the conversion in the OPO might show a slight delay after the start of to the pump pulse. It is interesting to note that the minimum laser pulse duration generated with the PPNL OPO laser is about two orders of magnitude shorter than those of the DF laser. The laser output in the experiments was 60 mW with a beam divergence of approximately 1 mrad. Calibrated attenuators enable us to control the laser irradiance levels on the camera over more than 4 orders of magnitude. The experiments were performed in an indoor test range of 300 m length. The maximum distance between the laser and the camera in the experiments was 275 m.

### 2.3. CMT camera and frequency doubled $CO_2$ laser

The CMT camera is described in section 2.1 above. The laser is a frequency doubled $CO_2$ laser providing a wavelength of 4.62 μm. The PRF is selectable between 2 and 105 kHz. The pulse length is 8.8 ns at 10 kHz, very similar to the PPLN OPO laser, and again much shorter than the DF laser pulses. The maximum power is 1.4 W at 100 kHz. The energy per pulse is 38 μJ at 10 kHz, yielding a maximum average power of 380 mW at 10 kHz. The optical path between the laser and the camera in the experiments was approximately 2 to 3 m as shown in figure 2. The maximum laser irradiance measured in front of the camera lens is 100 $\mu W/cm^2$, which is 10 times the maximum irradiance used in the DF laser experiments. Due to the short pulse duration, the maximum energy per pulse of 0.01 $\mu J/cm^2$ is 100 to 1000 times higher the maximum energy per pulse for the DF laser experiments.

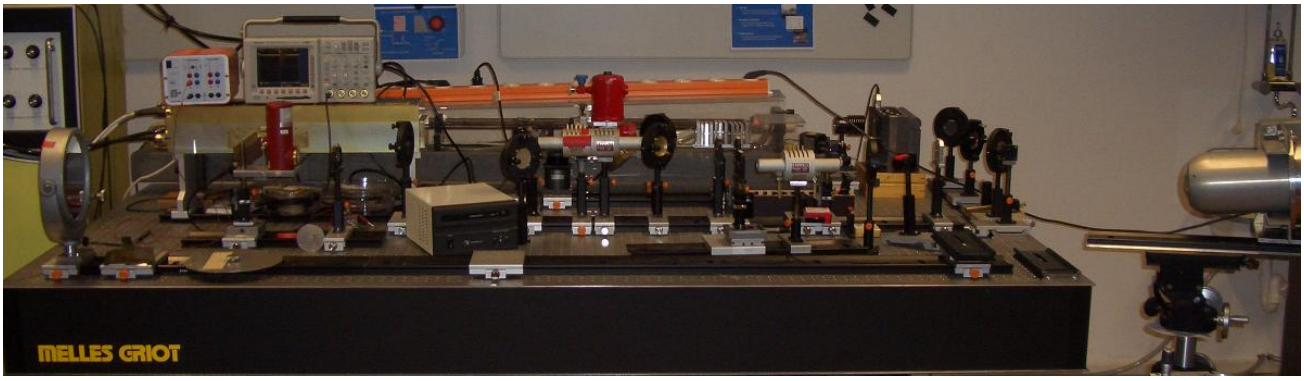


Figure 2: Frequency doubled $CO_2$ laser set-up with the CMT Imaging Seeker Simulator camera on the right

## 3. DAZZLING EXPERIMENTS

### 3.1. Area of saturated area versus laser irradiance.

In previous work on laser dazzling (reference 1) we have analysed the relation between the diameter of the saturated area and the laser irradiance. In figure 3 we show images of the CMT camera irradiated with the DF laser, for different irradiance levels. It was shown that the growth of the saturated area followed the envelope of the point spread function (PSF) for diffraction limited circular optics. The most important conclusion was that the diameter of the saturated area is proportional to $I_0^{1/3}$, where $I_0$ is the irradiance of the laser on the entrance optics. It is shown in reference 1 that the intensity level at the edges of the saturated area is determined by the wings of the point spread function. When $I_{sat}$ is the threshold irradiance for saturation, the radius of the saturated area can than be written as:

$$x_{sat} = \sqrt[3]{\frac{4}{\pi}\left(\frac{I_0}{I_{sat}}\right)} \qquad (1)$$

As an example we show the fit of this relation to the experimental data for the CMT camera and the DF laser in figure 4. The large diamonds in figure 4 mark the estimates for the saturation threshold level for a single pixel, following two different calculation methods as described in reference 1.

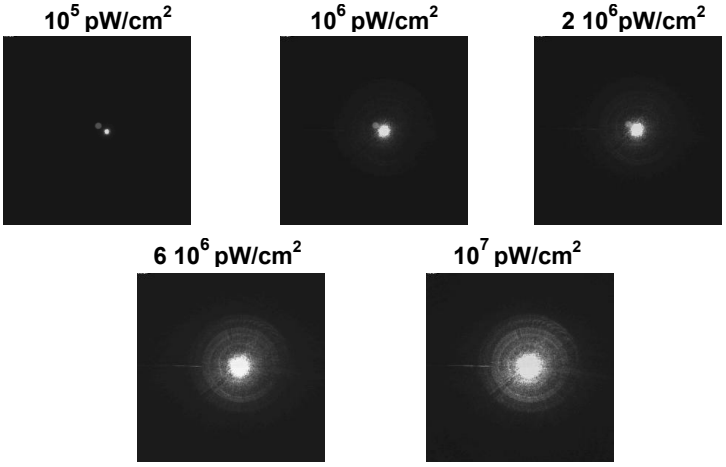


Figure 3: Impact of various DF laser irradiance levels on the CMT camera image (CW power)

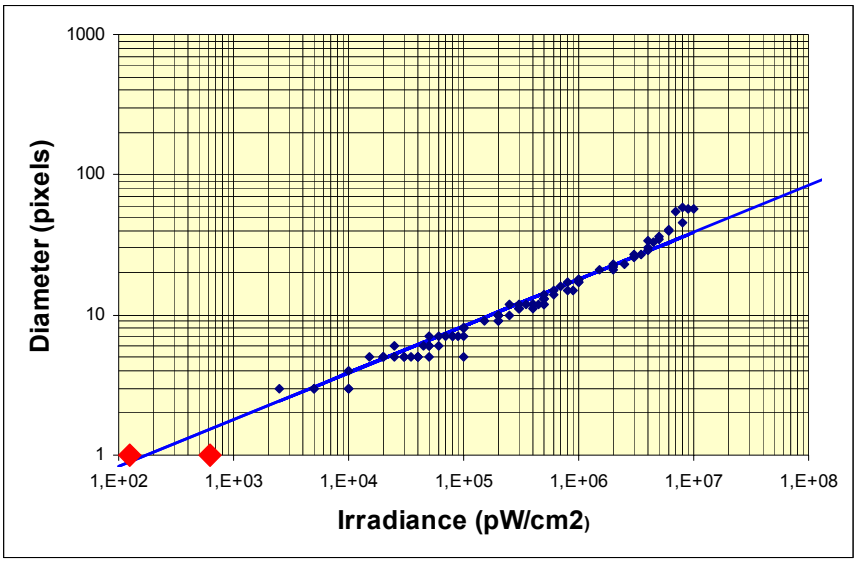


Figure 4: Observed laser dazzle area diameter in the CMT camera image as a function of DF laser irradiance. The blue curve follows the expression in equation 1.

In figure 5 we show images of the InSb camera irradiated by the PPLN OPO laser for different irradiance levels. The images shown are collected for the camera set in the narrow field of view mode and with the laser positioned in the centre of the field of view. Additional data were collected for the wide field of view mode and for 1° and 3° off-centre laser positions. Also for the data set of this camera, including the off-bore sight images, the growth of the saturated area can be described by equation 1. Effects of internal reflections or ghost images did not significantly disturb this.

If we have a closer look at the images in figure 5 we observe that for the higher laser irradiance levels, the saturated area is no longer uniformly saturated in the centre of the laser spot. This is even more clearly illustrated in an enlarged camera image in figure 6. In the central part of the dazzle area we no longer observe the maximum grey level in the image as we did for the lower irradiance levels. Apparently there is a non-linear behaviour in the detector which seems to decrease the detector output for very high intensities.

This non-linear behaviour is not only observed for maximum irradiance but also for observed for 10x (neutral density 1.0) lower intensity levels. Despite this non-linear behaviour the growth of the dazzled area continues to follow the relation given in equation 1. We explain this by observing that close to the edges of the saturated area, the intensity level on the detector array is not very far above the saturation level and therefore apparently still in the linear regime.

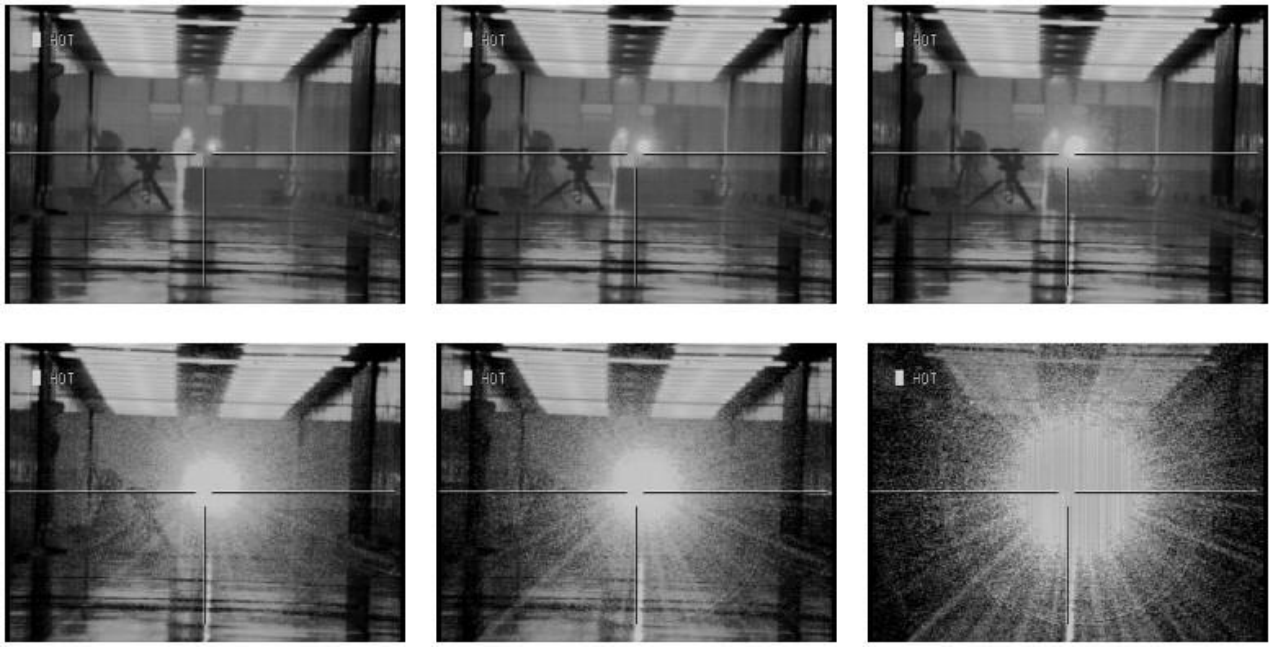


Figure 5: Impact of various laser irradiance levels on the narrow field of view InSb camera image. Laser attenuation levels in neutral density: 4.4, 3.3, 2.6 top left to right, 1.3, 0.6, 0.0 bottom left to right.

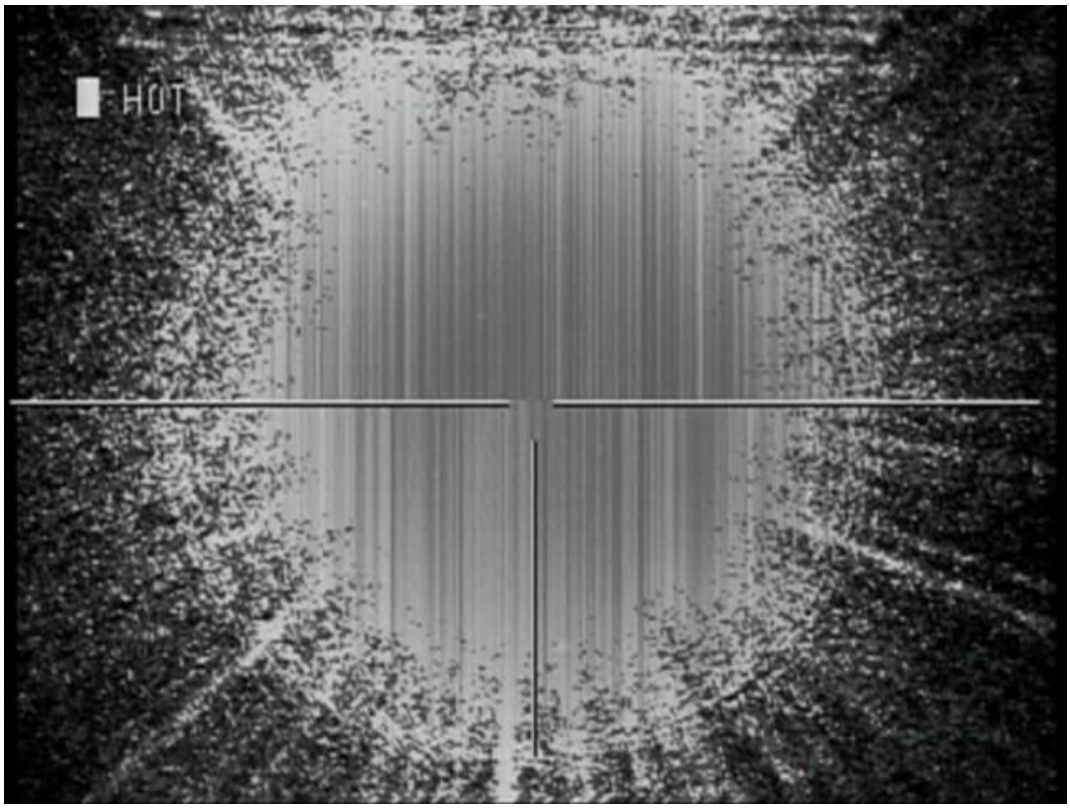


Figure 6: Observed laser dazzle image in the InSb camera, for high power short pulse (9 ns) irradiance.

## 3.2. Effects of high power pulses

The non-linear behaviour described in the previous section was not observed in the experiments with the DF laser and the CMT camera. This stimulated further work on the CMT camera with short laser pulses using frequency doubled $CO_2$ laser. This laser allows 10 times more average power, compared to the DF laser experiments, and initially it was intended to obtain some extra data points between $10^7$ and $10^8$ pW/cm$^2$ (10-100 µW/cm$^2$) in the graph in figure 4. The main difference however, is that the DF laser is limited to relatively long pulses between 5 µs and 100 µs and the $CO_2$ laser generates pulses 1000 to 10000 times shorter. This allows exploring the effects of much higher energy levels per pulse.

In the first experiments it was checked whether a sequence of short pulses at relatively low energy per pulse could generate an equivalent average power, while staying in the linear response of the detector array. This was done by increasing the number of laser pulses during the 1 ms integration time of the camera, keeping the energy per pulse constant. The laser was attenuated with neutral density filters to avoid saturation at the higher pulse repetition rate. The results are presented in figure 7. Each panel shows a detector grey level image and the corresponding intensity level scan through the centre of the laser spot.

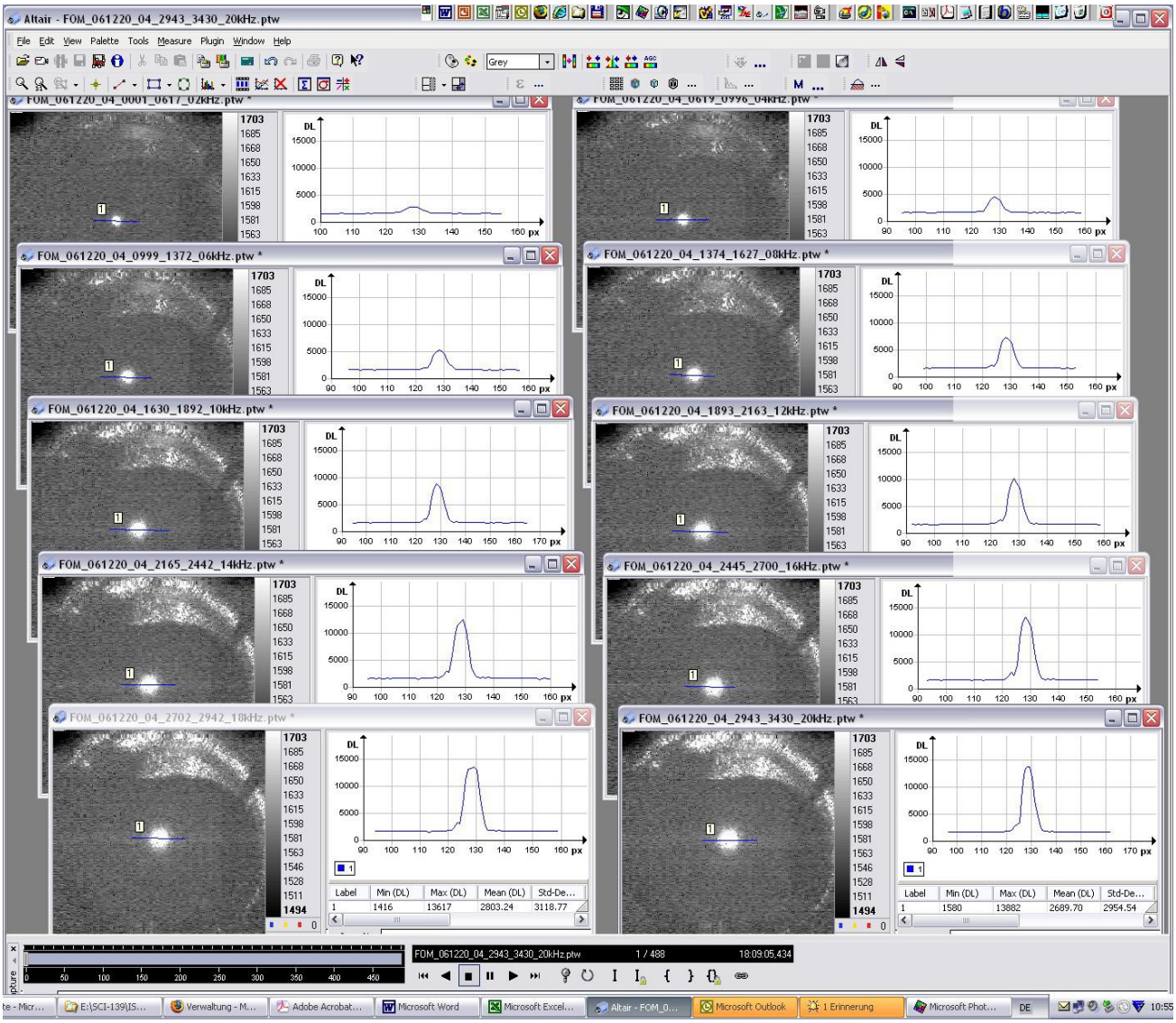


Figure 7: Laser illuminated images in the CMT camera, while increasing the pulse repetition frequency from 2 kHz (upper left) to 20 kHz (bottom right). For each image the corresponding intensity level scan through the centre of the laser spot is shown.

For the pulse peak levels in the different panels in figure 7 we observe a linear intensity increase from approximately 1000 to 11000 digital levels (DL) when the pulse repetition frequency is increased from 2 to 20 kHz, thus increasing the number of pulses during one image frame integration time from 2 to 20. The width of the pulse at half maximum remains the same. Note that all the images are displayed in the same dynamic range. The maximum intensity of the centre of the laser spot is outside this range in each of the images. The conclusion from this experiment is that in this "low-energy" pulse regime the sequence of pulses can replace a continuous source with the equivalent average power, to generate the same detector response.

The images in figure 7 were all collected using a 5000 times reduction compared top maximum power. In the next experiment the 10 kHz setting was taken as a starting point and the attenuators were subsequently removed. The results are shown in figure 8. The power levels are 0.0002, 0.001, 0.006, 0.033, 0.18 and 1.0 times the maximum power, from left to right and top to bottom. Again all the images are displayed in the same dynamic range. For the first step one would expect an increase of the peak height by a factor of 5, but in fact the peak only broadens and decreases in height. The image intensity saturation level of 16000 DL is never reached. The same is true for the next step in reduction of attenuation. A negative slope in the response curve is observed: the peak height decreases with increasing power. For the next steps we observe still no saturation, but at the same time we observe an area around the centre laser spot with an increased grey level. The size of this area increases with increasing power, but the grey level remains more or less constant. These observations indicate a non-linear response of the detector array to the short pulse high intensity laser illumination. Although InSb is a different material with different material properties, we observe that the non-linear behaviour in the InSb images starts at about the same irradiance levels as for the CMT camera.

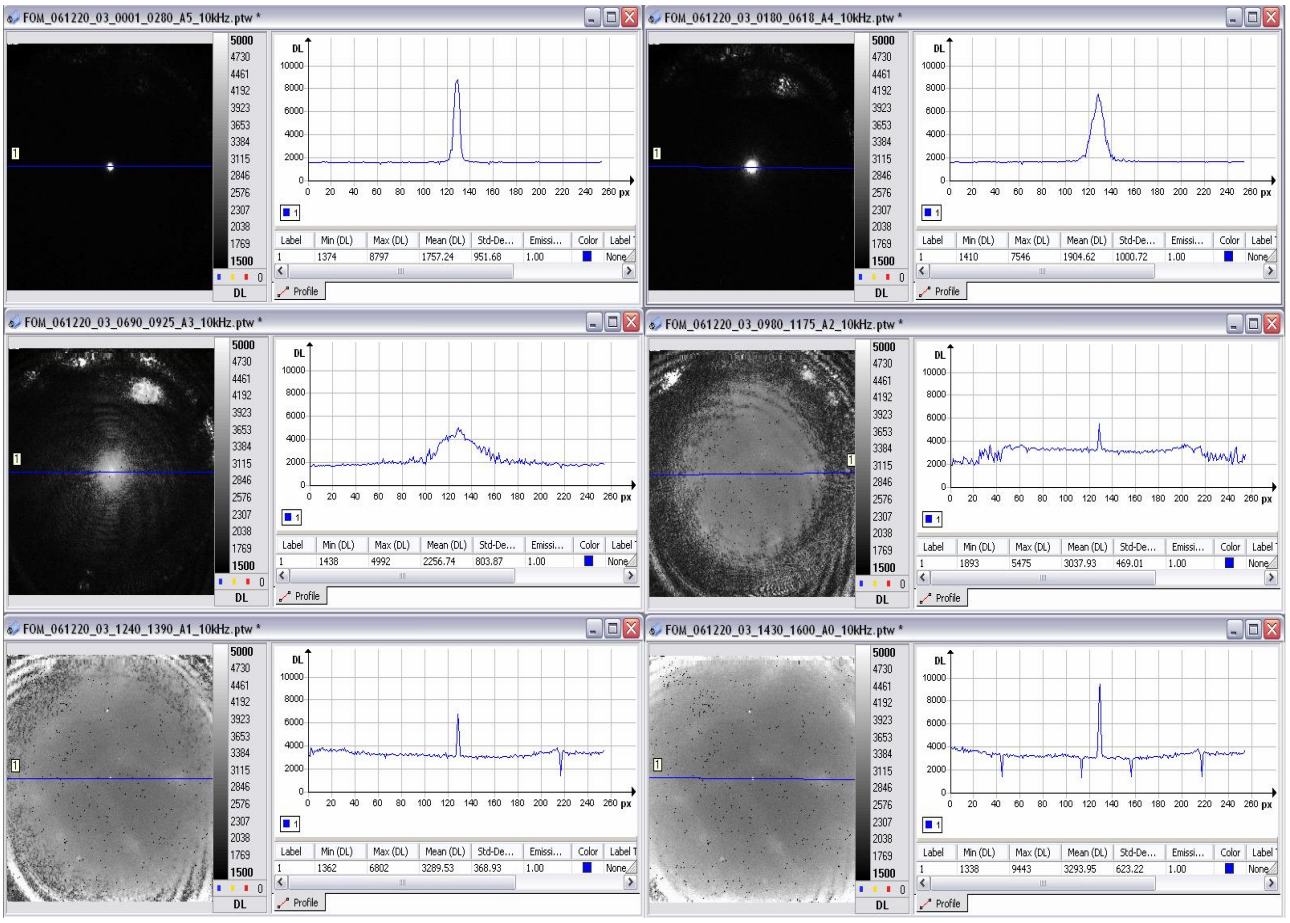


Figure 8: Laser illuminated images in the CMT camera, while increasing the irradiance to maximum irradiance from left to right and top to bottom: 0.0002, 0.001, 0.006, 0.033, 0.18 and 1.0 times maximum power respectively. For each image the corresponding intensity level scan through the centre of the laser spot is shown.

## 4. DISCUSSION OF NON-LINEAR EFFECTS

The origin of this non-linear behaviour is not obvious. Although quite an extensive number of papers has been published on laser damage, only a few papers in open literature mention these non-destructive non-linear in relation to laser countermeasures (reference 5). We group the reversible non-linear high intensity effects in the detector material in three categories: a) optical saturation, b) electrical saturation and c) device saturation. These effects can further be influenced by thermal effects induced by absorption of the laser irradiance. We will not consider saturation effects in the read-out circuit here.

We define optical saturation as effects in the photon-electron conversion, which cause an increase in photon absorption not resulting in an increase in detector output. Such a mechanism is free carrier absorption, where carriers excited from the valence band to the conduction band can be further excited to higher levels in the conduction band by absorption of photons (reference 6). Only above a certain optical intensity, their density becomes sufficient to produce a measurable contribution to the total absorption. Another optical effect causing a non linear increase of absorption is the carrier avalanche multiplication. Above a threshold in optical intensity, free carriers created by excitation across the band gap can acquire enough energy in the optical electric field strength to create additional carriers by impact ionisation. The result is an avalanche multiplication of free carriers. In first approach however, both effects will not show a negative slope in the response curve and it is therefore less likely that we can attribute the experimental observations to these effects.

Electrical saturation effects are effects which occur when large densities of photo-electrons are generated and these large electron densities enable saturation processes which limit the detector response. Electro-hole recombination is such an effect. As a first approach the direct-recombination rate is proportional to the number of available electrons in the conduction band and the number of holes in the valence band (reference 7). Vest and Grantham (reference 8) studied the response of a silicon photodiode to pulsed radiation and they show that the integrated-charge responsivity of the photodiode has a dependence on pulse energy. They observed a decrease in integrated-charge responsivity with increased pulse energy and attribute this to the increased concentration of majority carriers which decreases the direct recombination time at high incident pulse energies. This decrease in integrated-charge responsivity starts at pulse energies in the range between 0.1 and 1 μW and becomes stronger for higher pulse energies. In reference 9 Vest et al. show that the integrated-charge responsivity is a function of the total pulse energy, independent of the pulse length over the range from 60 ns to 1 μs. The authors of reference 9 speculate that there may be significant changes at pulse lengths longer than a few microseconds, where the incident pulse length exceeds the impulse response time of the silicon photodiode. The actual recombination rate will also depend on the detector design, because the recombination time competes with the time required for the carriers to cross the depletion region which depends on carrier mobility, depletion region width and junction potential.

By device saturation we refer to screening of the internal electric field of a photodiode by the large numbers of photo-generated charge carriers at high optical power. This results in photocurrent saturation. The screening of the internal electric field decreases the velocity of the photo-carriers and hence their transit time, which leads to reduction of the photodiode response. The basics of screening are described in text books like reference 10. Konno et al. (reference 11) studied the influence of photo-generated carriers of the internal electric fields in silicon.

Based on the discussion above we suggest that the non-linear effects are caused by a combination of electrical saturation and device saturation. All the material parameters involved, like recombination rate, drift velocity, mobility depend on temperature. An increase of temperature of the photodiode material due to absorption of high intensity laser radiation will therefore have an additional effect on the non-linear detector behaviour.

## 5. CONSEQUENCES FOR COUNTERMEASURE LASERS

### 5.1. Missile seekers

When applying lasers as a countermeasure, we have the intention to generate a response of a photo-detector which is much stronger than a given target signature. The target is a continuous source and the detector continuously receives a photon flux from the target. Countermeasure lasers are usually pulsed devices. We have discussed in this paper that for relatively low laser pulse energy we can approximate the detector response by considering the laser as a CW source with

a power equal to the pulse energy averaged over time. For high energy pulses this is no longer true and the CW approach will no longer provide good predictions of the detector response.

When the detector is hit by a short high energy laser pulse causing saturation, the question to be answered is how long the detector remains saturated after the laser pulse. If the detector shows a fast recovery within a fraction of the detector integration time, then the detector still "sees" the target signal most of the time. In that case we need more laser power to reach the jamming to target ratio, required to achieve the desired countermeasure result.

Not only for focal plane array seekers but also for first generation reticule seekers saturation effects can be important. If the detector shows a slow recovery, than the saturation of the detector can impact the bandwidth. This can influence the transfer function and reticule-generated frequencies can get distorted, leading to guidance degradation. It should be noted that the reticule is normally in the focal plane and the infrared detector is out-of-focus. This spreads the laser power over a larger area compared to the sharp laser spots on focal plane detectors, thus potentially reducing the saturation effects.

## 5.2. Laser sources

To avoid or to reduce the detrimental effects of photodiode saturation by putting all the laser energy in very short pulses, one would require longer laser pulses with reduced peak power. Countermeasure lasers use non-linear conversion processes to generate light in the wavelength band for which the seekers are sensitive. This conversion process is highly non-linear and using a lower peak power reduces the conversion efficiency. In a typical countermeasure laser source high repetition rate pump laser sources are used with pulse lengths of a few ns.

The peak powers in countermeasure lasers based on PPLN non-linear crystals are already considerably reduced compared to low repetition rate lasers. The attractiveness of PPLN is based in part on its large nonlinear coefficient, which enables the efficient frequency conversion of low-peak-power lasers (such as diode lasers and diode-pumped solid state lasers). However, continuous wave PPLN based lasers have been reported as well (reference 13) and therefore it should be possible to generate countermeasure lasers with pulse lengths considerably longer than a 5 to 10 ns. These continuous wave PPLN lasers make use of longer PPLN crystals (50 mm instead of 20 or 30 mm).

Whether a suitable countermeasure laser with longer pulse lengths can be made depends on how the non-linear conversion depends on pump pulse length. This is a complicated question that depends on many factors.

In order to better understand the consequences of the observed non-linear detector response on the effectiveness of laser countermeasures and in order to decide whether one can mitigate these effects by changing the choice of the laser design, one needs a broader investigation of the combinations of physical mechanisms causing these non-linear effects in detector devices.

# 6. CONCLUSION

In this paper we have shown experimental results of laser dazzling effects in infrared focal plane array cameras with different detector materials. It has been shown for these cameras that the increase of the saturated area with increasing laser irradiance is independent of the read-out circuit over a large dynamic range. An equation based on the optical point spread function is used to predict the size of the saturated area as a function of the laser irradiance at the front optics.

The experimental results for short pulses with high energy levels per pulse show a strong non-linear response of the detector arrays. Some physical processes potentially responsible for these effects are described, but the observed effects cannot be attributed to one single mechanism and are probably caused by a mix of effects. The potential consequences of this non-linear detector behaviour for the effectiveness of laser countermeasures applying short high energy pulses are discussed. At this moment we cannot draw any final conclusions except that for a better understanding of the consequences of the observed effects on laser countermeasures, one needs a broader investigation of the response of infrared detectors to short high energy laser pulses. This will then allow changing the laser design in order to mitigate these effects.

## 7. ACKNOWLEDGEMENT

The authors would like to thank their colleagues of NATO SCI-139 for their support and discussions on this topic. The TNO contribution to this work was performed as a part of the TNO research programme V408 on Electronic Warfare for Platform Protection for the Royal Netherlands Air Force sponsored by the Netherlands MoD. The contributions form FGAN-FOM and CELAR were sponsored by the MoDs from the Germany and France respectively.

## REFERENCES

1. Ric (H.)M.A. Schleijpen, J.C. van den Heuvel, A.L. Mieremet , B. Mellier, F.J.M. van Putten: “Laser Dazzling of Focal plane Array Cameras”, SPIE Vol. 6543-48, Infrared Imaging Systems: Design, Analysis, Modeling, and Testing XVIII, Orlando April 2007.
2. H.M.A. Schleijpen, S.R. Carpenter, B. Mellier, A. Dimmeler: “Imaging Seeker Surrogate for IRCM evaluation”, SPIE Vol 6397-16: Technologies for Optical Countermeasures III, Stockholm, September 2006.
3. V. Lavigne, B. Ricard, “Fast Risley prisms camera steering system: calibration and image distortion correction through the use of a three-dimensional refraction model”, Opt. Eng. 46(4), 043201-1 1038-1047 April 2007.
4. H.H.P.Th. Bekman, J.C. van den Heuvel, F.J.M van Putten, H.M.A. Schleijpen, “Development of a Mid-Infrared Laser for Directed Infrared Countermeasures”, Technologies for Optical Countermeasures, London, SPIE Vol. 5615-03.
5. L.J. Cox, M. A. Batten, S.R. Carpenter, P.A.B. Saddleton: “Modelling countermeasures to imaging infrared seekers”, Technologies for Optical Countermeasures, London, SPIE Vol. 5615-12.
6. M v Allmen, “Coupling of laser radiation to metals and semiconductors in M Bertolotti (ed.) NATO Advanced Institute, Series B: Physics, Vol 84, Plenum Press New York 1983.
7. S. M. Sze, Semiconductor Devices Physics and Technology, (John Wiley & Sons, New York, 1985).
8. R. E. Vest and S. Grantham, "Response of a silicon photodiode to pulsed radiation," Appl. Opt.Vol. 42, 5054 (2003).
9. R. E. Vest, S. B. Hill, and S. Grantham, "Saturation effects in solid-state photodiodes and impact on EUVL pulse energy measurements," Metrologia Vol. 43, S84-S88 (2006).
10. C. Kittel, Solid State Physics, (John Wiley & Sons, New York, 1976).
11. K. Konno, O. Matsushima, D. Navarro, and M. Miura-Mattausch, "Limit of validity of the drift-diffusion approximation for simulation of photodiode characteristics," Appl Phys Lett., Vol. 84, 1398 (2004).
12. A. Villange, T Brudevoll, K Stenersen, “IR laser induced heating in $Hg_{0.72}Cd_{0.28}Te$”, SPIE Vol. 6397-13: Technologies for Optical Countermeasures III, Stockholm, September 2006.
13. Arisholm, G., Stenersen, K., Rustad, G., Lippert, E., and Haakestad, M. “Mid-Infrared optical paramagnetic oscillators based on periodically-poled lithium niobate”. FFI/Rapport-2002/02830, 2002 Kjeller, Norway.